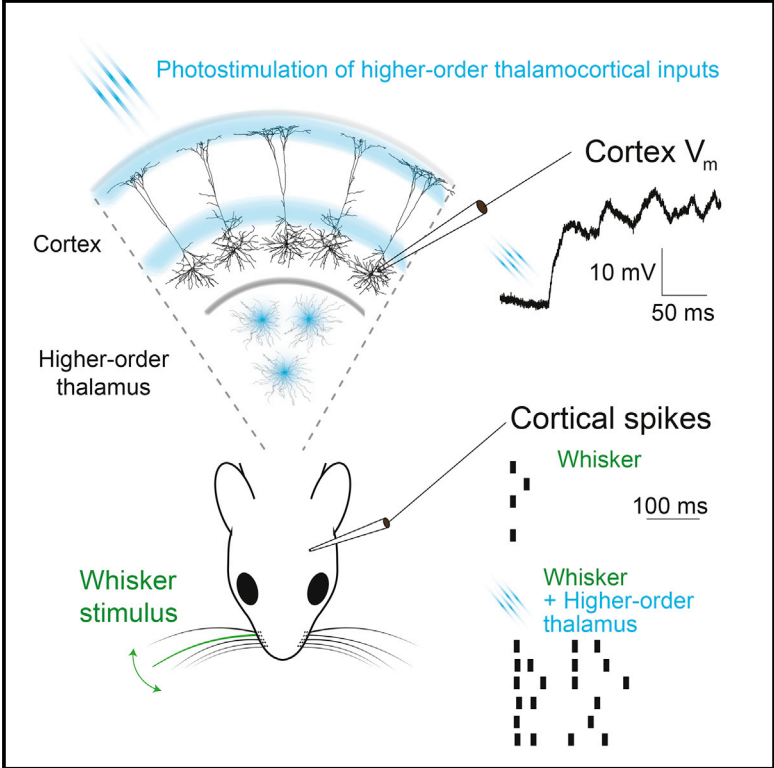


## Cortical Sensory Responses Are Enhanced by the Higher-Order Thalamus

### Graphical Abstract



### Authors

Rebecca A. Mease, Markus Metz, Alexander Groh

### Correspondence

alexander.groh@gmail.com

### In Brief

Mease et al. investigate a major, yet puzzling, thalamocortical pathway from the higher-order thalamus to the cortex. This pathway enhances sensory responses in layer 5 cortical neurons on fast and slow timescales. Such enhancement of cortical responses by higher-order thalamocortical inputs may serve to specifically amplify relevant sensory content.

### Highlights

- Effect of the higher-order thalamus on cortical sensory processing is investigated
- Cortical neurons in layer 5 integrate inputs from two parallel thalamic pathways
- Higher-order thalamus enhances cortical responses on fast and slow timescales

# Cortical Sensory Responses Are Enhanced by the Higher-Order Thalamus

Rebecca A. Mease,<sup>1</sup> Markus Metz,<sup>1</sup> and Alexander Groh<sup>2,\*</sup>

<sup>1</sup>Institute for Neuroscience, Technische Universität München, Biedersteiner Straße 29, 80802 Munich, Germany

<sup>2</sup>Department of Neurosurgery, Klinikum rechts der Isar, Technische Universität München, Ismaninger Straße 22, 81675 Munich, Germany

\*Correspondence: [alexander.groh@gmail.com](mailto:alexander.groh@gmail.com)

<http://dx.doi.org/10.1016/j.celrep.2015.12.026>

This is an open access article under the CC BY-NC-ND license (<http://creativecommons.org/licenses/by-nc-nd/4.0/>).

## SUMMARY

In the mammalian brain, thalamic signals reach the cortex via two major routes: primary and higher-order thalamocortical pathways. While primary thalamocortical nuclei transmit sensory signals from the periphery, the function of higher-order thalamocortical projections remains enigmatic, in particular their role in sensory processing in the cortex. Here, by optogenetically controlling the thalamocortical pathway from the higher-order posteromedial thalamic nucleus (POM) during whisker stimulation, we demonstrate the integration of the two thalamocortical streams by single pyramidal neurons in layer 5 (L5) of the mouse barrel cortex under anesthesia. We report that POM input mainly enhances sub- and suprathreshold activity via net depolarization. Sensory enhancement is accompanied by prolongation of cortical responses over long (800-ms) periods after whisker stimulation. Thus, POM amplifies and temporally sustains cortical sensory signals, possibly serving to accentuate highly relevant sensory information.

## INTRODUCTION

The higher-order thalamus consists of an enigmatic class of thalamic nuclei defined by dominating “driver” input from the cortex. In the rodent whisker system, the higher-order nucleus is the posterior medial thalamic nucleus (POM), which extensively innervates large parts of the cortex, including primary and secondary somatosensory cortices, the motor cortex, and association cortices (Deschênes et al., 1998; Wimmer et al., 2010) (Figure 1A). Despite this widespread innervation, the functional impact of POM (e.g., suppression or enhancement) on sensory processing in the cortex is not known.

Based on POM’s thalamocortical (TC) projection targets in cortical layer 1 (L1) and L5A in barrel cortex (BC) (Koralek et al., 1988; Lu and Lin, 1993; Wimmer et al., 2010), POM may monosynaptically excite pyramidal neurons (Rubio-Garrido et al., 2009; Meyer et al., 2010) and/or provide disinhibitory inhibition through putative synapses with GABAergic neurons, in particular in L1. However, anatomical studies (Koralek et al., 1988; Lu and Lin, 1993; Rubio-Garrido et al., 2009; Wimmer

et al., 2010) and predictions based on overlap of dendrites and boutons as a proxy for contacts (Meyer et al., 2010) cannot reveal the sign of synaptic inputs or their effect on cortical dynamics.

The excitatory role of POM TC inputs was demonstrated in brain slices by (Bureau et al., 2006; Petreanu et al., 2009; Theyel et al., 2010; Viaene et al., 2011). Petreanu et al. first stimulated channelrhodopsin-2 (ChR2)-expressing POM boutons and found that responses were dependent on both the cell type and the subcellular location of the inputs. Recently, POM-evoked excitation has been shown in BC L2/3 neurons in vivo (Gambino et al., 2014; Jouhannau et al., 2014). The putative indirect inhibitory action of POM can be inferred solely from POM’s dense projections to L1, which contains inhibitory neurons and pyramidal tufts (Jiang et al., 2013). While synapses between POM and inhibitory neurons have not been demonstrated, TC projections to L1 are of general interest in understanding cortical computations such as gain control (Larkum et al., 1999, 2004) and temporal binding mechanisms (Llinas et al., 2002).

As a first approach to understand the role of POM on sensory responses in the BC in vivo, we studied the putative enhancer and/or suppressor role of POM by recording whisker responses from BC L5 neurons in isoflurane anesthetized mice while optogenetically stimulating POM boutons. We chose L5 neurons because (1) the majority of L5 neurons receive functional TC input (Bureau et al., 2006), and (2) both L5A and L5B pyramidal subtypes have dendrites in POM’s principal target layers, L1 and L5A, and were predicted to be the primary recipients of POM inputs in terms of estimated synapse counts (Meyer et al., 2010). Furthermore, as recipients of functional input from both ventral posteromedial nucleus (VPM) and POM (Viaene et al., 2011), L5 neurons have been suggested to play a key role in integrating L1 “context” with sensory “content” to form sensory percepts (Llinas et al., 2002; Larkum, 2013).

Despite this wealth of data about the POM-cortex pathway, the effect of POM on whisker responses in BC is unknown. To quantify how POM affects cortical sensory processing, we paired POM bouton stimulation with whisker stimulation and in vivo electrophysiology. POM stimulation in combination with sensory stimulation enhanced spiking in the majority of L5 neurons. Notably, this enhancement of sensory responses was sustained over long (~800-ms) periods. Lastly, intracellular recordings revealed excitatory inputs from POM, which integrate with whisker-evoked excitatory potentials in both L5 cell types. Together, the data show a net enhancing rather than a

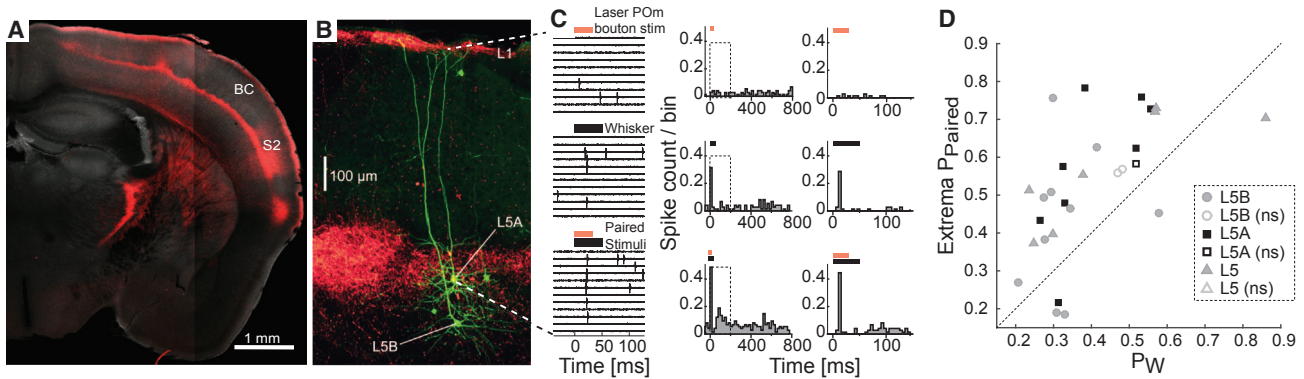


**Figure 1. Modulation of Whisker Responses in L5 Neurons in BC by POM Bouton Activation**

(A) Expression of ChR2-mCherry in POM neurons resulted in widespread axonal and bouton labeling (red) of several cortical areas. BC and other cortical areas are densely innervated in L1 and L5. Other cortical areas, for example S2, are additionally innervated in L4. Light activation of POM boutons was targeted to BC. Visible lines are due to imperfect tile alignment and a drop in pixel intensities toward the edges.

(B) Example fluorescence image of single L5A and L5B neurons (green) in BC and projections from POM (red). Neurons were filled with biocytin after each juxtosomal experiment or during intracellular recordings and then visualized with Streptavidin/Alexa Fluor 647 and DAB.

(C) Left: examples of a L5A neuron's spike responses to POM bouton stimulation by light activation of ChR2 (red bar, upper), whisker stimulation (black bar, middle), and paired whisker and POM stimulation (bottom). Middle: corresponding PSTHs (−50 to 800 ms, 20-ms bins). Note enhanced early and late responses after paired stimulation. The early response (200 ms, dashed box) was used to summarize the POM effect for all neurons in (D). Right: same as middle at higher time resolution: −20 to 150 ms (5-ms bins).

(D)  $P_{\text{paired}}$  versus  $P_{\text{w}}$  for all juxtosomal recordings ( $n = 28$ ) within 200 ms following stimulation. Out of seven stimulation conditions with varying delays, the condition with the strongest effect on  $P_{\text{w}}$  is shown. This extremum was either enhancement ( $n = 23$ ) or suppression ( $n = 5$ ). Each marker corresponds to one neuron; filled markers show significant change ( $n = 25/28$ ) of  $P_{\text{w}}$  by POM and open markers indicate unchanged neurons,  $\chi^2$  test. Neurons were classified as L5B (gray circle,  $n = 12$ ), L5A (black square,  $n = 9$ ), or unrecovered L5 neurons (gray triangles,  $n = 7$ ).

suppressing function of POM on sensory responses in L5 neurons in BC, demonstrating in vivo cortical coincidence detection of parallel TC inputs.

## RESULTS

### Optogenetic Stimulation of POM Boutons in Barrel Cortex Boosts Sensory Responses in the Majority of L5 Neurons

The basic experiment to study the effect of POM inputs on whisker responses in L5 of BC during anesthesia is illustrated in Figure 1. After expressing ChR2-mCherry in POM neurons, we found extensive labeling of several cortical areas (Figures 1A and S1), demonstrating widespread innervation of cortical L1 and L5 by POM. POM-specific control was achieved by optogenetic stimulation of boutons expressing ChR2-mCherry (Petreanu et al., 2007) in the mouse BC under isoflurane anesthesia. The photostimulus was delivered via a fiber optic (diameter = 125  $\mu\text{m}$ ) positioned  $\sim 300 \mu\text{m}$  above and perpendicular to the cortical surface (pulse length = 30 ms, power density = 32–58  $\text{mW}/\text{mm}^2$ ). We recorded whisker and POM responses in single L5A and L5B neurons in BC, in either juxtosomal or whole-cell patch clamp configuration (Figure 1B). Whiskers were deflected by air puffs or using a piezo wafer (see Supplemental Experimental Procedures). While we found whisker responsive and unresponsive neurons intermingled in L5, only responsive neurons were tested for interactions between sensory responses and POM bouton stimulation. Correct targeting of virus injections to POM was verified by post hoc histology of the injection site and the characteristic POM projections bands

in L1 and L5A in BC (Figures 1A, 1B, and S1; Lu and Lin, 1993; Wimmer et al., 2010). Classification into L5A and L5B was done as described previously (Groh et al., 2010; Groh and Krieger, 2013) and described in detail in Supplemental Experimental Procedures and Figure S1.

The first dataset consists of 28 juxtosomal L5 recordings, the majority of which were recovered and classified as L5A or L5B ( $n = 9$  and  $n = 12$ , respectively; see Experimental Procedures). The remaining recordings were classified as L5 ( $n = 7$ ), based on recording depths (620–750  $\mu\text{m}$  from pia). To study the effect of POM input on sensory responses in L5, we compared spiking responses during 200 ms following different combinations of stimulation: (1) whisker deflection, (2) photostimulation of POM boutons, and (3) paired stimulation of whiskers and POM boutons (Figure 1C).

POM bouton stimulation alone did not affect spontaneous spiking probabilities ( $P_{\text{spont}}$ ) under these conditions, except in a minority (5/28) of cells: two L5A neurons for which  $P_{\text{spont}}$  increased from 0.19 to 0.37 and 0.28 to 0.56, two L5B neurons for which  $P_{\text{spont}}$  increased from 0.05 to 0.08 and 0.14 to 0.2, and one unrecovered L5 neuron for which  $P_{\text{spont}}$  increased from 0.14 to 0.31 ( $p < 0.05$ ,  $\chi^2$  test; see Figure S2A). However, spike responses were more reliably evoked for higher photostimulation intensities (Figure S2B), demonstrating that the spike-driving capability of POM depends on the strength of stimulation.

Pairing POM bouton stimulation with whisker deflections typically enhanced sensory responses in L5 neurons (Figure 1C). 25 out of 28 neurons showed response probability for paired POM and whisker stimulation ( $P_{\text{paired}}$ ) significantly different than response probability for whisker stimulation ( $P_{\text{w}}$ ) alone.

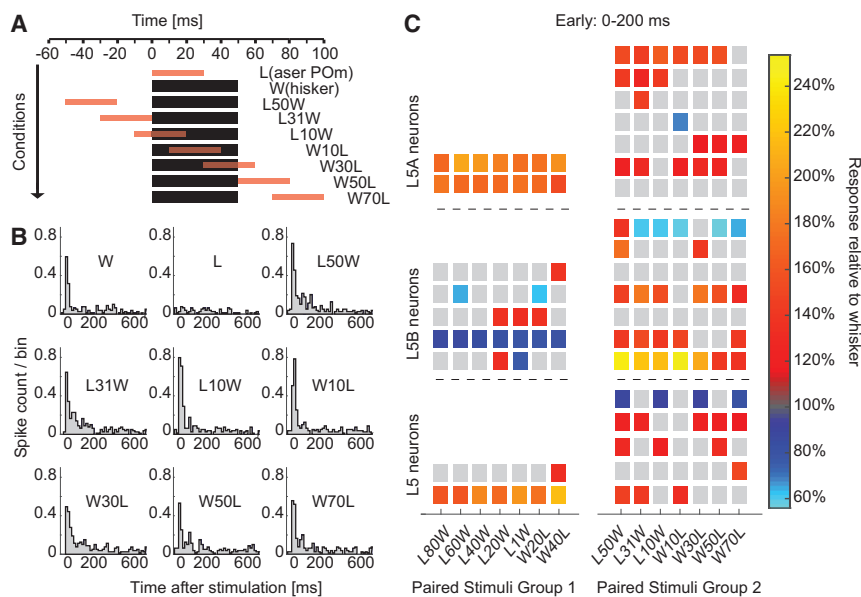


**Figure 2. In Vivo L5 Cortical Responses to Whisker Stimulation Are Typically Enhanced by POM Bouton Stimulation**

(A) Schematic showing the relative timing between the two stimuli: whisker deflection (black) and POM bouton stimulation (red). The different conditions were: whisker deflection (“W”), POM bouton (laser [“L”]), or paired stimulation with seven delays between whisker and POM bouton stimulation. For example, in the first paired condition, the POM stimulus preceded the whisker deflection by 50 ms (“L50W”). Stimulus delay group 2 is shown.

(B) Example PSTHs from a L5A juxtosomal recording of spike responses to different stimulation conditions: 20-ms bins, 79 trials. POM bouton stimulation significantly enhanced  $P_W$  for L50W, L31W, and L10W, with a maximum of 142% of  $P_W$ . (C) Integration windows for the juxtosomal dataset, L5A ( $n = 9$ ), L5B ( $n = 12$ ), and unrecovered L5 neurons ( $n = 7$ ) separated by the dashed lines. Two different timing protocols (“Paired Stimuli Groups”) are shown in the left and right columns; condition names on x axis are as in A. Each row in a column represents one neuron; colored squares indicate significantly different  $P_{Paired}$  compared to  $P_W$ . Fill

color indicates relative change to whisker response probability, warm ( $>100\%$ ) or cool ( $<100\%$ ) colors indicate enhancement or suppression of whisker responses by POM.  $\chi^2$  test, significance at  $p < 0.05$ ; gray squares show conditions for which  $P_{Paired}$  was not significantly different from  $P_W$ .

We determined the maximal effect for each neuron from a range of delays between whisker and POM bouton stimulation. The maximal effect was either the maximal percentage increase or decrease in  $P_{Paired}$  relative to  $P_W$ , calculated as  $100 * P_{Paired} / P_W$ . In the rare case ( $n = 2$ ) that both increases and decreases were seen in the same cell, the largest absolute change was reported as the maximum. L5 neurons with enhanced whisker responses significantly outnumbered those with suppressed whisker responses by a factor of 4 (20 enhanced and 5 suppressed neurons,  $p < 0.05$ , binomial test; mean enhancement and suppression to  $157\% \pm 34\%$  and  $70\% \pm 11\%$  of  $P_W$ , respectively). An example suppressed neuron is shown in Figure S2C.

Figure 1D summarizes this effect: 7 out of 9 identified L5A neurons were enhanced to a mean of  $155\% \pm 29\%$  of  $P_W$  (1 unchanged, 1 suppressed to 68%,  $\chi^2$  test), 7 out of 12 identified L5B neurons were enhanced to a mean of  $166\% \pm 43\%$  of  $P_W$  (2 unchanged, 3 suppressed to a mean  $65\% \pm 12\%$ ,  $\chi^2$  test), and 6 out of 7 unrecovered L5 neurons were enhanced to a mean of  $150\% \pm 34\%$  of  $P_W$  (1 suppressed to 88%). The POM effect strength varied between individual experiments (Figure 1D), and we correlated the effect strength to the estimated expression level of Chr2-mCherry for each cell. These data suggest that the differences in expression levels across experiments contributed to the observed variability (Figure S3).

We next characterized the temporal structure of integration windows for paired POM and whisker stimulation on a cell-by-cell basis (Figure 2), using a similar stimulus pairing approach as in Groh et al. (2013). For each L5 neuron, we systematically varied the timing of sensory responses relative to POM bouton stimulation over a range of relative time delays: POM bouton stimulation preceding the whisker by 80 ms (“L80W”) and whisker stimulation preceding POM stimulation by 70 ms (“W70L”) (Figure 2A). Paired stimulation increased spiking

compared to whisker stimulation alone, and the degree of increase varied with the relative timing of the stimuli (Figure 2B). In this example, 3 out of 7 paired conditions resulted in  $P_{Paired}$  significantly greater than  $P_W$ , with a maximal effect of 142% of  $P_W$ .

To summarize the data for all 28 recordings, we plotted enhancement and suppression for all delay conditions in which  $P_{Paired}$  was significantly different than  $P_W$  (Figure 2C). Together, the data support the tendency of POM input to enhance, rather than suppress whisker responses in L5 neurons in BC. The integration windows (number of significant pairings) were variable across the group of recorded neurons and often encoded the paired stimulus over the entire range of times tested, suggesting that the actual integration window may extend for longer than 80 ms. The fraction of enhanced neurons was greater for L5A than L5B (L5A: 7/9, L5B: 7/12), suggesting slightly more effective enhancement of L5A sensory responses.

### POM Stimulation Prolongs Whisker Responses

POM evokes long-lasting “plateau” potentials in L2/3 neurons (Gambino et al., 2014), raising the possibility that POM can lengthen sensory responses in the cortex. Indeed, the PSTHs in Figures 3A and 1C show L5B responses that substantially outlast stimulus duration for paired conditions. To quantify POM-mediated lengthening of whisker responses, we plotted maximum  $P_{Paired}$  versus  $P_W$  for all 28 neurons, calculated in a time window starting 200 ms and ending 800 ms after the stimulation (the “late response phase”; Figure 3B). While POM bouton stimulation alone did not affect  $P_{spont}$  ( $p < 0.05$ ,  $\chi^2$  test), pairing POM bouton stimulation with whisker deflections significantly increased the probability of late L5 sensory responses. This analysis is summarized on a cell-by-cell basis in Figure 3B by plotting  $P_{Paired}$  versus  $P_W$ : 7 out of 9 L5A neurons

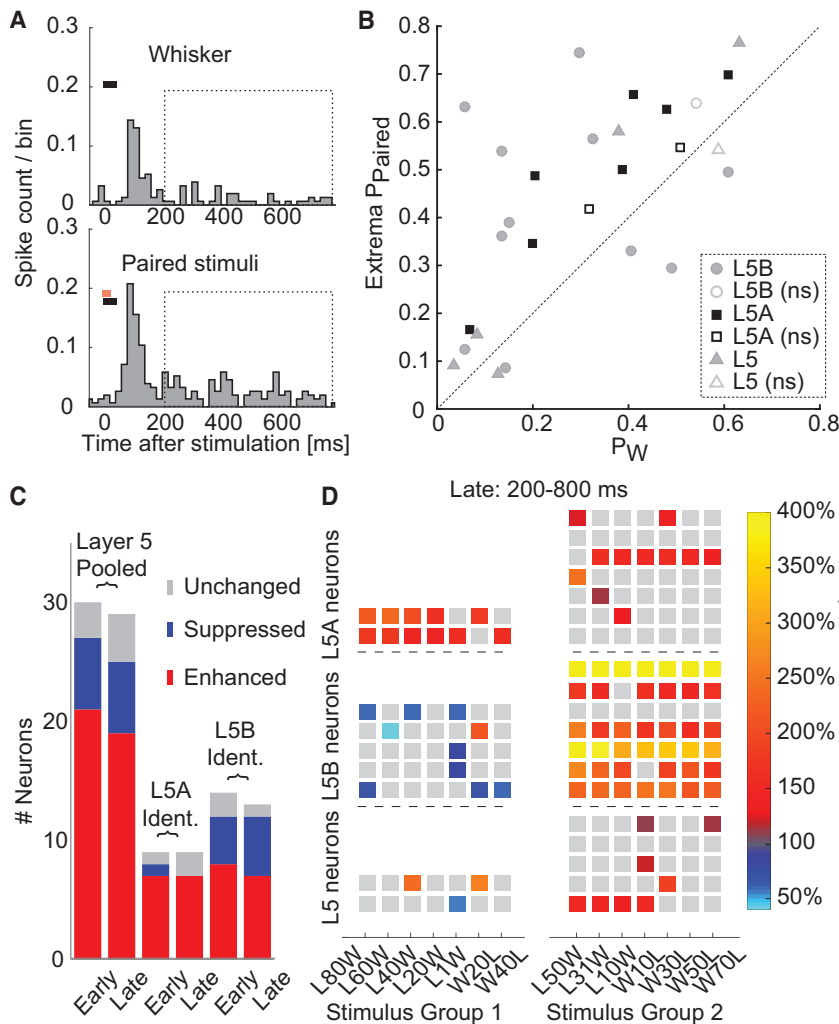


**Figure 3. POM Bouton Stimulation Prolongs Whisker Responses**

(A) Example PSTHs of a L5B neuron in response to whisker (upper panel) or paired whisker + POM stimulation (lower panel), with 20-ms bins. Note increased spiking 200–800 ms after paired stimulation (boxed region, also compare to Figure 1C). Late  $P_W$  (200–800 ms) were significantly enhanced in response to all paired stimulation conditions, with a maximum of 259% of  $P_W$ .

(B)  $P_{paired}$  versus  $P_W$  for all juxtatasomal recordings ( $n = 28$ ) during the late response phase (200–800 ms, boxed region in A). Out of seven stimulation conditions, the condition with the strongest effect on  $P_W$  is shown. The extremum was either enhancement ( $n = 22$ ) or suppression ( $n = 6$ ). Each marker corresponds to one neuron. Filled markers indicate neurons for which POM stimulation significantly changed  $P_W$  ( $n = 24$ ) and open markers indicate unchanged neurons ( $n = 4$ );  $\chi^2$  test. L5B (gray circle,  $n = 12$ ), L5A (black square,  $n = 9$ ), unrecovered L5 neurons (gray triangles,  $n = 7$ ).

(C) Summary of POM’s effect on whisker responses in L5 neurons ( $n = 28$ ) for early and late responses: “Unchanged,” “Suppressed,” and “Enhanced.” Neurons were classified into L5A ( $n = 9$ ), L5B ( $n = 12$ ), and unrecovered L5 neurons ( $n = 7$ ); the category “Layer 5” contains all L5 neurons ( $n = 28$ ). A small minority of neurons were both enhanced and suppressed, depending on the delay condition, and were assigned to both enhanced and suppressed for this summary plot ( $n = 2$  for early and  $n = 1$  for late response phase). In all groups, the majority of neurons had enhanced whisker responses during early and late response phases. The fraction of enhanced versus suppressed neurons was greatest in the L5A group (L5A early: 7/1 and L5A late: 7/0; L5B early: 8/4 and L5B late: 7/5).

(D) Integration windows for the late response phase (200–800 ms). L5A ( $n = 9$ ), L5B ( $n = 12$ ), and unrecovered L5 neurons ( $n = 7$ ) separated by dashed

line. The same timing protocols (“Paired Stimuli Groups”) as in Figure 2C were used and are shown in the left and right columns. Each row in a column represents one neuron; colored squares indicate  $P_{paired}$  significantly different from  $P_W$ . Plotting conventions as in Figure 2C.

were enhanced to an average of  $170\% \pm 52\%$  of  $P_W$  (2 unchanged,  $\chi^2$  test), 7 out of 12 L5B neurons were enhanced to an average of  $260\% \pm 75\%$  of  $P_W$ , or suppressed ( $n = 4$ ) to an average of  $71\% \pm 12\%$  of  $P_W$  (1 unchanged,  $\chi^2$  test), and 5/7 uncategorized L5 neurons were enhanced to an average of  $167\% \pm 59\%$  of  $P_W$  (1 suppressed to 57%, 1 unchanged,  $\chi^2$  test). Thus, while late enhancement was significantly stronger for L5B than for L5A neurons (rank sum test,  $p < 0.05$ ), a subset of L5B neurons was also slightly suppressed. Pooling all neurons, the ratio of enhanced to suppressed neurons was nearly the same as for the early response phase (19 enhanced and 5 suppressed,  $p < 0.05$  binomial test; mean effects of  $200\% \pm 74\%$  and  $69\% \pm 12\%$ , respectively). Figure 3C summarizes the effect of POM activation on early and late whisker response components for all recordings.

The integration windows for the late phase of the response 200–800 ms after stimulation are shown in Figure 3D. While the late enhancement or suppression effect was variable across

neurons, a substantial fraction (9/28) of L5 neurons showed robust enhancement to all or nearly all paired conditions.

### POM Enhancement of Whisker-Evoked Subthreshold Responses

We observed suppression of whisker responses in only a minority (<20%) of recorded neurons. This rarity of suppression was somewhat surprising given POM’s dense projection band in L1 and needed to be confirmed directly with intracellular recordings.

Figure 4A shows intracellular post-synaptic potential (PSP) responses to POM bouton stimulation for six example L5 neurons (see Figure S4A for all 21 recordings). Responses to POM bouton activation typically occurred with short latency (4–6 ms), suggesting a monosynaptic origin via activation of POM–L5 synapses with our standard stimulation intensity (PSP characteristics and cell-by-cell PSP analysis in Figures 4B and S4B, respectively,  $n = 10$  L5A, 11 L5B). However, some neurons (2/10 L5A,

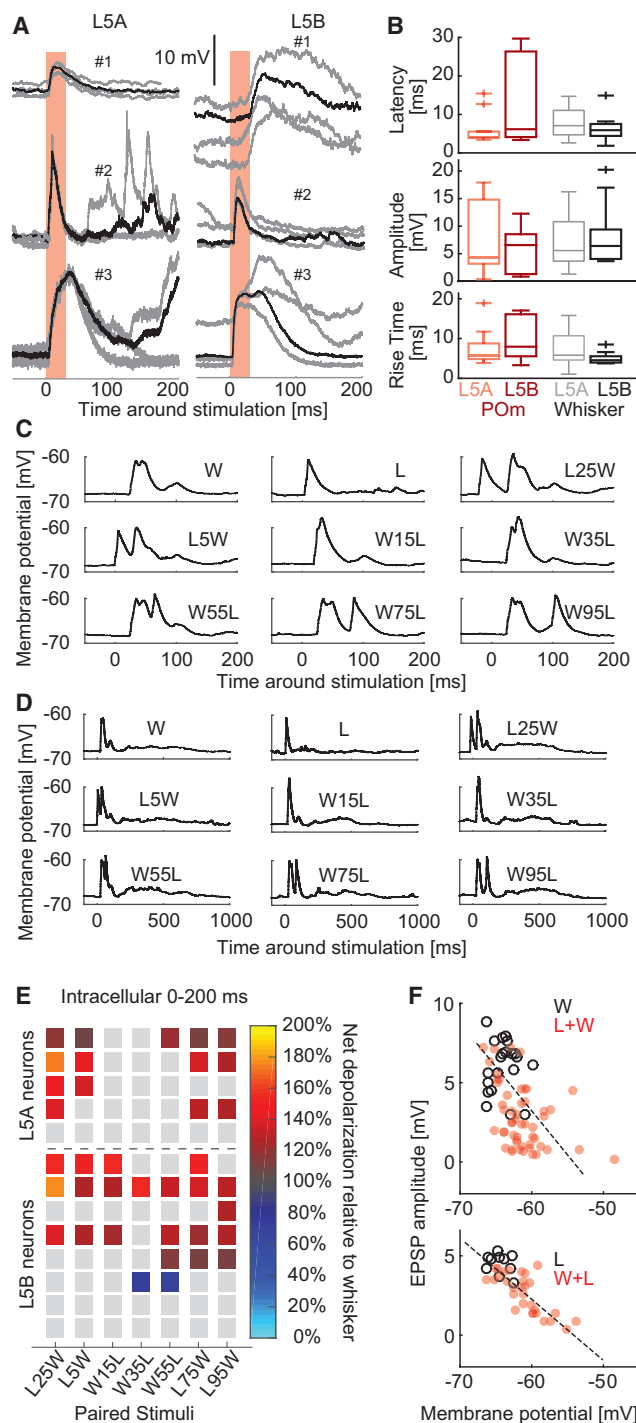


**Figure 4. POM Bouton Stimulation Boosts Whisker-Evoked EPSPs**

(A) Example whole-cell patch clamp recordings of PSPs evoked by POM bouton stimulation (red) from three L5A (left) and three L5B (right) neurons (resting membrane potentials of  $-64$ ,  $-70$ , and  $-72$  mV and  $-60$ ,  $-66$ , and  $-67$  mV for L5A#1–3 and L5B#1–3, respectively). Gray traces are single-trial examples, and black traces show the median response for each neuron from 11–34 repetitions.

(B) Box plot summary of POM and whisker-evoked PSP latency (upper), maximum amplitude (middle), and 10%–90% rise time (lower) for L5A ( $n = 10$ )

and L5B ( $n = 11$ ) intracellular recordings. Box plots show medians, interquartile ranges, and outliers (“+”). Unpooled data from individual neurons are presented in Figure S4B. Whisker-evoked EPSP latencies are approximated based on offset estimates of the delay between puff trigger and the actual whisker deflection ( $\sim 22$  ms, see Experimental Procedures). (C) Example whole-cell patch-clamp recording of a L5A neuron during whisker stimulation (W) or POM bouton stimulation (L) or paired whisker and POM bouton stimulation at different delays. Traces show averages from eight repetitions. Whisker EPSPs contain on and off components following the caudal and rostral deflections by air puffs. (D) Same as in (C); a longer time period is shown to illustrate delayed depolarization. (E) Integration windows for the intracellular dataset for the early response phase 0–200 ms after stimulation. The net depolarization was calculated as the integral of the baseline-corrected average membrane potential trace. Each row in a column represents one neuron; colored squares indicate significantly different net depolarization compared to whisker stimulation alone (rank sum test). Fill color indicates relative change to whisker-evoked net depolarization. Plotting conventions as in Figures 2C and 3D. (F) Correlation between evoked EPSP amplitude and preceding membrane potential for whisker-evoked EPSPs following POM stimulation (upper) and POM-evoked EPSPs following whisker stimulation (lower). For this L5A neuron, correlation coefficients were  $r = -0.50$  and  $r = -0.79$ , respectively. Responses to individual stimuli are shown in black (“W” or “L”) and pooled paired stimuli in red (“L+W” or “W+L”).

For a subset of recordings (5 L5A, 8 L5B), we examined sub-threshold responses to paired whisker and POM bouton stimulation at different relative time delays. All conditions, including POM bouton stimulation alone, triggered excitatory PSP (EPSP) responses with short and long timescales (Figures 4C and 4D, respectively) corresponding to the early and late responses observed in the juxtosomal recordings (Figure 3).

To quantify the interactions between POM- and whisker-evoked EPSPs, we compared the net depolarization for each stimulus condition to the whisker-evoked net depolarization. The net depolarization was calculated as the integral of the baseline-corrected average membrane potential trace. We found that 9 of 13 neurons (4 L5A, 5 L5B) showed whisker responses significantly enhanced (an increase in net depolarization) by POM stimulation for at least one delay condition. Enhancement was most commonly seen for more extreme delay conditions. Three neurons did not show any significant change and only one neuron showed a significant decrease in net depolarization for paired stimuli, suggesting that in this L5B neuron whisker EPSPs were shunted by POM input (Figure 4C).

and L5B ( $n = 11$ ) intracellular recordings. Box plots show medians, interquartile ranges, and outliers (“+”). Unpooled data from individual neurons are presented in Figure S4B. Whisker-evoked EPSP latencies are approximated based on offset estimates of the delay between puff trigger and the actual whisker deflection ( $\sim 22$  ms, see Experimental Procedures).

(C) Example whole-cell patch-clamp recording of a L5A neuron during whisker stimulation (W) or POM bouton stimulation (L) or paired whisker and POM bouton stimulation at different delays. Traces show averages from eight repetitions. Whisker EPSPs contain on and off components following the caudal and rostral deflections by air puffs.

(D) Same as in (C); a longer time period is shown to illustrate delayed depolarization.

(E) Integration windows for the intracellular dataset for the early response phase 0–200 ms after stimulation. The net depolarization was calculated as the integral of the baseline-corrected average membrane potential trace. Each row in a column represents one neuron; colored squares indicate significantly different net depolarization compared to whisker stimulation alone (rank sum test). Fill color indicates relative change to whisker-evoked net depolarization. Plotting conventions as in Figures 2C and 3D.

(F) Correlation between evoked EPSP amplitude and preceding membrane potential for whisker-evoked EPSPs following POM stimulation (upper) and POM-evoked EPSPs following whisker stimulation (lower). For this L5A neuron, correlation coefficients were  $r = -0.50$  and  $r = -0.79$ , respectively. Responses to individual stimuli are shown in black (“W” or “L”) and pooled paired stimuli in red (“L+W” or “W+L”).

For near-simultaneous whisker and POM stimulation, the response to the second stimulus was markedly smaller in amplitude than the response to the same stimulus in isolation (for example, Figure 4C, middle row). We evaluated how responses evoked by the first stimulus affected the responses evoked by the second stimulus by calculating the correlation coefficient  $r$  between trial-by-trial evoked EPSP amplitude and pre-EPSP membrane potential (Crochet et al., 2011) (Figure 4F; note that response amplitudes for second stimuli approach 0 mV). Significant negative correlation was observed between (1) whisker-evoked EPSP amplitude and preceding POM-evoked depolarization (5/7 L5B and 3/5 L5A neurons;  $r$  median:  $-0.56$ , first quartile:  $-0.80$ , third quartile:  $-0.50$ ) and (2) POM-evoked EPSP amplitude and preceding whisker-evoked depolarization (7/7 L5B and 4/5 L5A neurons;  $r$  median:  $-0.70$ , first quartile:  $-0.86$ , third quartile:  $-0.46$ ). This interaction is consistent with either the same glutamatergic inputs being activated by POM and whisker stimulation or with POM evoking mixtures of excitation and inhibition. Nevertheless, given the increase in net depolarization in paired whisker and POM stimulation conditions, the whole-cell experiments support the view that POM's net impact on L5 whisker responses is excitatory and that only a minority of neurons are suppressed.

## DISCUSSION

Studies of POM input to cortical neurons *in vivo* are rare (Gambino et al., 2014; Jouhanneau et al., 2014) and have not addressed the effects of POM on cortical sensory responses. The present study investigated the impact of POM inputs on whisker responses in L5 BC of anesthetized mice. Juxtacellular and intracellular data in combination with optogenetic activation of POM inputs demonstrate that TC signals from primary thalamus (VPM) are integrated with higher-order TC signals from POM, resulting in a general enhancement and prolongation of cortical sensory responses.

### Enhancement of Sensory Responses via Depolarization

The enhancement of sensory signals in L5 neurons was mediated by POM-evoked depolarization (Figure 4). POM-evoked EPSPs of varying magnitudes were observed in all intracellular recordings (Figure S4A). Such POM excitatory input to pyramidal neurons of BC was first shown by Bureau et al. (2006) and subsequently confirmed (Petreanu et al., 2009; Theyel et al., 2010; Mao et al., 2011; Viaene et al., 2011; Gambino et al., 2014; Jouhanneau et al., 2014). We find here that such POM-evoked events can combine with whisker-evoked EPSPs (Figure S4A) to increase net depolarization (Figure 4).

The absence of POM-evoked IPSPs was somewhat surprising, given the dense POM projection to cortical L1, which contains inhibitory neurons. POM-mediated inhibition was also not found in previous studies (Theyel et al., 2010; Viaene et al., 2011; Gambino et al., 2014; Jouhanneau et al., 2014). Nonetheless, our study does not rule out the possibility of some POM-mediated inhibition, for several reasons. First, somatic voltage recordings and current injections *in vivo* prohibit robust conclusions about the voltage in distal dendrites, where POM-mediated inhibition may be expected. Thus, while inhibition was not de-

tected with POM stimulation alone (Figures 4A and S4A), the interaction of POM- and whisker-evoked EPSPs (Figure 4F) is consistent with POM pushing the whisker response toward the GABA reversal potential, as a result of putative POM synapses with L1 interneurons. Second, inhibitory neurons may be tonically active at high rates during anesthesia, rendering additional optogenetically triggered, POM-mediated inhibition ineffective. Finally, POM-evoked inhibition may work on timescales slower than were sampled in our pairing intervals.

In order to more generally understand POM's effect on cortical dynamics, it will be necessary to study POM input to other cortical areas *in vivo*, as large region-specific differences are expected. For example, the projection pattern and synaptic properties of POM input to the secondary somatosensory cortex (S2) (Viaene et al., 2011) predict a much stronger POM effect on sensory responses in S2. In fact, POM effectively drives spikes in S2 in the slice (Theyel et al., 2010). In contrast, in BC, POM stimulation alone rarely evoked spikes using our standard stimulation (see also Viaene et al., 2011; Gambino et al., 2014; Jouhanneau et al., 2014). However, the capability of POM to drive cortical spikes was dependent on the strength of the stimulus, as L5 spikes could be evoked by stronger ( $>2\text{--}3\times$  laser power) POM stimulation (Figure S2B). Thus, given enough synchronized activation—e.g., in the awake animal, in which POM is quite active (Moore et al., 2015; Urbain et al., 2015)—POM may contribute to spiking in BC, even in the absence of concurrent sensory stimulation.

### Prolongation of Sensory Responses

The long effect of POM stimulation on L5 sensory responses (Figure 3) represents an important foundation for future understanding of the function of higher-order thalamic nuclei. Mechanistically, this sustained activity could be due to properties of POM synapses, as well as recurrent network activity in the L5B-POM-L5 loop, and evidence for both mechanisms exists.

POM inputs specifically activate mGluR potentials in L5 neurons (Viaene et al., 2011), which last for several hundred milliseconds. Furthermore, long-lasting POM-evoked potentials in L2/3 neurons have recently been shown *in vivo* (Gambino et al., 2014). These plateau potentials are mediated by NMDA currents, and, taken together with this present study, it is tempting to hypothesize that NMDA potentials are driven by coincident activity of the two TC pathways, “higher-order” POM and “primary” VPM, resulting in characteristic dendritic “Ca<sup>2+</sup> spikes” in L5 (Yuste et al., 1994; Schiller et al., 1997). A role for L5B in coupling columnar input with L1 input was suggested as a cellular mechanism underlying perception (Linias et al., 2002; Larkum, 2013). In this scheme, signals from POM arriving in cortical L1 would cause dendritic plateau potentials that increase AP output only when temporally coupled with additional activity arriving at different layers, for example, whisker signals via the VPM-L4 pathway (Larkum et al., 1999).

Along with long-timescale synaptic effects, sustained activity may arise from the putative recurrent cortico-thalamo-cortical loop circuitry between POM and L5. POM neurons are effectively driven by POM-projecting L5B neurons (Reichova and Sherman, 2004; Groh et al., 2008), and as suggested here and by Viaene et al. (2011), POM activity may be returned to L5B neurons.

Taken together, POM's effects on cortical activity—mGluR activation, NMDA activation, and putative L5-POM-L5 recurrent excitation—potentially serve to sustain sensory-evoked responses in TC networks. These long-timescale effects may be a fundamental feature of POM function.

While the role of POM in enhancing and prolonging sensory responses in the whisker system was unknown, a similar function has been demonstrated in the primate visual TC system by (Purushothaman et al., 2012). This study demonstrated that the higher-order pulvinar thalamic nucleus provides potent excitation to the visual cortex (V1), as inactivation of the pulvinar resulted in an almost complete suppression of V1 visual responses. Whether POM inactivation causes a similarly dramatic effect in BC is currently unknown, but these findings in combination with our data suggest that the excitatory effect of higher-order thalamus is neither modality nor species specific.

### L5 Subtype Specificity

Optogenetic stimulation of POM-BC synapses *in vitro* evoked larger excitatory responses in L5A than in L5B (Petreanu et al., 2009; Mao et al., 2011), predicting a subtype-specific effect of POM on whisker signals *in vivo*. While the present results are in general agreement with this prediction, as the fraction of enhanced L5A (7/9) neurons was greater than the fraction of L5B (7/12) neurons, we interpret the L5 subtype specificity of the sensory enhancement as rather moderate. Here, subtype-specific effects are possibly obscured by the *in vivo* stimulation paradigm. We likely activated POM boutons synchronously in both tuft and basal dendrites, in contrast to *in vitro* studies using pharmacological and optical approaches to stimulate inputs in a subcellular-specific manner (Petreanu et al., 2009; Mao et al., 2011). These approaches are currently not possible *in vivo*. Together with stronger ChR2 expression as a result of a new generation of ChR2, as well as a bias toward whisker responsive L5 neurons in our sample, these differences may explain why POM-evoked EPSPs were comparable in both cell types (Figures 4 and S4). However, our results are consistent with anatomical approximations based on bouton-dendrite overlap, predicting that L5A and L5B neurons are contacted by the same number of POM boutons (Meyer et al., 2010), as well as *in vitro* findings that both L5A and L5B neurons in BC are dually innervated by VPM and POM, and that responses to POM stimulation are similar in both cell types (Viaene et al., 2011).

### Putative Functional Implications of Cortical Enhancement via Higher-Order Thalamus

The function of POM on the level of perception, learning, and behavior is controversially discussed (Ahissar et al., 2000; Masri et al., 2009; Ahissar and Oram, 2015; Gambino et al., 2014; Moore et al., 2015; Urbain et al., 2015). In contrast, the role of higher-order thalamus in perception is arguably better understood in the primate visual system, in which the higher-order pulvinar nucleus is implicated in selective visual attention and visual salience (Rafal and Posner, 1987; Robinson and Petersen, 1992; Snow et al., 2009).

The amplification of cortical signals by higher-order thalamic output, as described here for the whisker system and previously for the visual system (Purushothaman et al., 2012), may “high-

light” sensory cues of particular relevance, such as sensory events that are in conflict with expectations. Given the long timescales of the effect in the case of POM, activity in this pathway may prime cortical networks for a behavioral response. This putative priming signal would be broadcast to the cortex via POM's widespread cortical innervation (Deschênes et al., 1998), thereby simultaneously increasing excitability of sensory, motor, and association cortices.

### EXPERIMENTAL PROCEDURES

All experiments were performed in accordance with institutional animal welfare guidelines and were approved by the state government of Bavaria, Germany. Single-neuron recordings in juxtacellular and whole-cell intracellular configuration were done in L5 BC in isoflurane anaesthetized adult wild-type mice using an ELC-01X amplifier (NPI Electronics). Expression of ChR2 was stereotaxically targeted to POM using virus-mediated gene transfer, which allowed fast optogenetic activation of POM boutons in BC using a custom-built fiberoptic laser setup. Whisker stimulation was done with air puff (intracellular data) or piezo deflections (most juxtacellular recordings) of the principal whisker. L5 neurons were classified as described earlier (Groh et al., 2010; Groh and Krieger, 2013). Data were recorded with Spike2 (CED) and analyzed with custom-written MATLAB software (MathWorks). A detailed description of experimental procedures is provided in Supplemental Experimental Procedures.

### SUPPLEMENTAL INFORMATION

Supplemental Information includes Supplemental Experimental Procedures, four figures, and one table and can be found with this article online at <http://dx.doi.org/10.1016/j.celrep.2015.12.026>.

### AUTHOR CONTRIBUTIONS

A.G. and M.M. conducted the experiments, A.G. designed the research and secured funding, and R.A.M. and A.G. analyzed the data and wrote the paper.

### ACKNOWLEDGMENTS

We thank Arthur Konnerth and Bert Sakmann for providing infrastructure and support at the Institute for Neuroscience at the TU München, Patrik Krieger, and Anton Sumser for comments on the manuscript, and Jackie Schiller for helpful comments on intracellular data. Funding was provided by the Deutsche Forschungsgemeinschaft Sachbeihilfe (GR 3757/1-1 and SFB 1158) and the Max Planck Society.

Received: August 6, 2015

Revised: September 27, 2015

Accepted: November 30, 2015

Published: December 31, 2015

### REFERENCES

- Ahissar, E., and Oram, T. (2015). Thalamic relay or cortico-thalamic processing? Old question, new answers. *Cereb Cortex* 25, 845–848.
- Ahissar, E., Sosnik, R., and Haidarliu, S. (2000). Transformation from temporal to rate coding in a somatosensory thalamocortical pathway. *Nature* 406, 302–306.
- Bureau, I., von Saint Paul, F., and Svoboda, K. (2006). Interdigitated paralemniscal and lemniscal pathways in the mouse barrel cortex. *PLoS Biol.* 4, e382.
- Crochet, S., Poulet, J.F., Kremer, Y., and Petersen, C.C. (2011). Synaptic mechanisms underlying sparse coding of active touch. *Neuron* 69, 1160–1175.
- Deschênes, M., Veinante, P., and Zhang, Z.W. (1998). The organization of corticothalamic projections: reciprocity versus parity. *Brain Res. Brain Res. Rev.* 28, 286–308.



- Gambino, F., Pagès, S., Kehayas, V., Baptista, D., Tatti, R., Carleton, A., and Holtmaat, A. (2014). Sensory-evoked LTP driven by dendritic plateau potentials in vivo. *Nature* *515*, 116–119.
- Groh, A., and Krieger, P. (2013). Structure-function analysis of genetically defined neuronal populations. *Cold Spring Harb. Protoc.* *2013*, 961–969.
- Groh, A., de Kock, C.P., Wimmer, V.C., Sakmann, B., and Kuner, T. (2008). Driver or coincidence detector: modal switch of a corticothalamic giant synapse controlled by spontaneous activity and short-term depression. *J. Neurosci.* *28*, 9652–9663.
- Groh, A., Meyer, H.S., Schmidt, E.F., Heintz, N., Sakmann, B., and Krieger, P. (2010). Cell-type specific properties of pyramidal neurons in neocortex underlying a layout that is modifiable depending on the cortical area. *Cereb. Cortex* *20*, 826–836.
- Groh, A., Bokor, H., Mease, R.A., Plattner, V.M., Hangya, B., Stroh, A., Deschênes, M., and Acsady, L. (2013). Convergence of cortical and sensory driver inputs on single thalamocortical cells. *Cereb. Cortex* *24*, 3167–3179.
- Jiang, X., Wang, G., Lee, A.J., Stornetta, R.L., and Zhu, J.J. (2013). The organization of two new cortical interneuronal circuits. *Nat. Neurosci.* *16*, 210–218.
- Jouhanneau, J.S., Ferrarese, L., Estebanez, L., Audette, N.J., Brecht, M., Barth, A.L., and Poulet, J.F. (2014). Cortical fosGFP expression reveals broad receptive field excitatory neurons targeted by POM. *Neuron* *84*, 1065–1078.
- Koralek, K.A., Jensen, K.F., and Killackey, H.P. (1988). Evidence for two complementary patterns of thalamic input to the rat somatosensory cortex. *Brain Res.* *463*, 346–351.
- Larkum, M. (2013). A cellular mechanism for cortical associations: an organizing principle for the cerebral cortex. *Trends Neurosci.* *36*, 141–151.
- Larkum, M.E., Zhu, J.J., and Sakmann, B. (1999). A new cellular mechanism for coupling inputs arriving at different cortical layers. *Nature* *398*, 338–341.
- Larkum, M.E., Senn, W., and Lüscher, H.R. (2004). Top-down dendritic input increases the gain of layer 5 pyramidal neurons. *Cereb. Cortex* *14*, 1059–1070.
- Llinas, R.R., Leznik, E., and Urbano, F.J. (2002). Temporal binding via cortical coincidence detection of specific and nonspecific thalamocortical inputs: a voltage-dependent dye-imaging study in mouse brain slices. *Proc. Natl. Acad. Sci. USA* *99*, 449–454.
- Lu, S.M., and Lin, R.C. (1993). Thalamic afferents of the rat barrel cortex: a light- and electron-microscopic study using Phaseolus vulgaris leucoagglutinin as an anterograde tracer. *Somatosens. Mot. Res.* *10*, 1–16.
- Mao, T., Kusefoglou, D., Hooks, B.M., Huber, D., Petreanu, L., and Svoboda, K. (2011). Long-range neuronal circuits underlying the interaction between sensory and motor cortex. *Neuron* *72*, 111–123.
- Masri, R., Quiton, R.L., Lucas, J.M., Murray, P.D., Thompson, S.M., and Keller, A. (2009). Zona incerta: a role in central pain. *J. Neurophysiol.* *102*, 181–191.
- Meyer, H.S., Wimmer, V.C., Hemberger, M., Bruno, R.M., de Kock, C.P., Frick, A., Sakmann, B., and Helmstaedter, M. (2010). Cell type-specific thalamic innervation in a column of rat vibrissal cortex. *Cereb. Cortex* *20*, 2287–2303.
- Moore, J.D., Mercer Lindsay, N., Deschênes, M., and Kleinfeld, D. (2015). Vibrissa Self-Motion and Touch Are Reliably Encoded along the Same Somatosensory Pathway from Brainstem through Thalamus. *PLoS Biol.* *13*, e1002253.
- Petreanu, L., Huber, D., Sobczyk, A., and Svoboda, K. (2007). Channelrhodopsin-2-assisted circuit mapping of long-range callosal projections. *Nat. Neurosci.* *10*, 663–668.
- Petreanu, L., Mao, T., Sternson, S.M., and Svoboda, K. (2009). The subcellular organization of neocortical excitatory connections. *Nature* *457*, 1142–1145.
- Purushothaman, G., Marion, R., Li, K., and Casagrande, V.A. (2012). Gating and control of primary visual cortex by pulvinar. *Nat. Neurosci.* *15*, 905–912.
- Rafal, R.D., and Posner, M.I. (1987). Deficits in human visual spatial attention following thalamic lesions. *Proc. Natl. Acad. Sci. USA* *84*, 7349–7353.
- Reichova, I., and Sherman, S.M. (2004). Somatosensory corticothalamic projections: distinguishing drivers from modulators. *J. Neurophysiol.* *92*, 2185–2197.
- Robinson, D.L., and Petersen, S.E. (1992). The pulvinar and visual salience. *Trends Neurosci.* *15*, 127–132.
- Rubio-Garrido, P., Pérez-de-Manzo, F., Porrero, C., Galazo, M.J., and Clascá, F. (2009). Thalamic input to distal apical dendrites in neocortical layer 1 is massive and highly convergent. *Cereb. Cortex* *19*, 2380–2395.
- Schiller, J., Schiller, Y., Stuart, G., and Sakmann, B. (1997). Calcium action potentials restricted to distal apical dendrites of rat neocortical pyramidal neurons. *J. Physiol.* *505*, 605–616.
- Snow, J.C., Allen, H.A., Rafal, R.D., and Humphreys, G.W. (2009). Impaired attentional selection following lesions to human pulvinar: evidence for homology between human and monkey. *Proc. Natl. Acad. Sci. USA* *106*, 4054–4059.
- Theyel, B.B., Llano, D.A., and Sherman, S.M. (2010). The corticothalamocortical circuit drives higher-order cortex in the mouse. *Nat. Neurosci.* *13*, 84–88.
- Urbain, N., Salin, P.A., Libourel, P.A., Comte, J.C., Gentet, L.J., and Petersen, C.C. (2015). Whisking-Related Changes in Neuronal Firing and Membrane Potential Dynamics in the Somatosensory Thalamus of Awake Mice. *Cell Rep.* *13*, 647–656.
- Viaene, A.N., Petrof, I., and Sherman, S.M. (2011). Properties of the thalamic projection from the posterior medial nucleus to primary and secondary somatosensory cortices in the mouse. *Proc. Natl. Acad. Sci. USA* *108*, 18156–18161.
- Wimmer, V.C., Bruno, R.M., de Kock, C.P., Kuner, T., and Sakmann, B. (2010). Dimensions of a projection column and architecture of VPM and POM axons in rat vibrissal cortex. *Cereb. Cortex* *20*, 2265–2276.
- Yuste, R., Gutnick, M.J., Saar, D., Delaney, K.R., and Tank, D.W. (1994). Ca<sup>2+</sup> accumulations in dendrites of neocortical pyramidal neurons: an apical band and evidence for two functional compartments. *Neuron* *13*, 23–43.